*Journal of Materials and Manufacturing (2023) 1: 11-20*

JMM Materials and Manufacturing Journal of Materials and Manufacturing

# Parametric optimization and evaluating mechanical properties of poly lactic acid proceed by FDM additive manufacturing

Aamer Sharif[a]*, Hashim Khan[a], Najma Bashir[b], Waqas Alam[c]

[a]*Department of Mechanical Engineering, Cecos University of IT and Emerging Science, Peshawar, Pakistan*
(ORCID: 0000-0003-1571-8675), aamirsharif120@gmail.com,
(ORCID: 0009-0007-8751-6788), hashimkhan@cecos.edu.pk
[b]*Department of Physics, Riphah International University Lahore, Pakistan*
(ORCID: 0000-0003-3149-6902), najmabashir20@gmail.com
[c]*School of Mechanical Engineeing, Purdue University, USA*
(ORCID: 0009-0009-8240-8731), *alamw@purdue.edu*

**Abstract**

Additive manufacturing is an emerging technique for creating 3-D objects from a component's design. The current work focuses on evaluating PLA's mechanical properties through Fused deposition modeling (FDM) techniques. The optimization was carried out by varying the printing processes parameters such as printing speed (60 mm/s, 100 mm/s, and 140 mm/s), layer thickness (0.1 mm, 0.2 mm, and 0.3 mm), and infill density (40%, 60%, and 80%). The impact of printing parameters on impact strength can be considered for the optimization process. The L9 orthogonal array was used to prepare the samples, and the Taguchi optimization method was used to optimize the process condition. Moreover, the current study includes an ANOVA of the measured data that determines the significance and assesses the total impact of each input parameter on response. The result shows that impact strength is higher at an infill density of 80%, a minimum layer thickness of 0.1 mm, and a printing speed of 100 Cº. Furthermore, the ANOVA study shows that the order of the parameters that affected the impact strength was infill density followed by layer thickness and printing speed.

*Keywords:* Additive manufacturing, Fused deposition modeling, PLA, Layer thickness, Infill density, Printing speed.

| **Nomenclature** | |
|---|---|
| $d_i$ | infill density |
| $l_t$ | layer thickness |
| $s_p$ | printing speed |
| $s_i$ | impact strength |

## 1. Introduction

Additive Manufacturing (AM) process covers a wide range of technologies, including Fused Deposition Modeling (FDM). FDM is the most widely used AM method because it is safe, affordable, easy to operate, and used in various materials [1]. Using the FDM technique, complex geometries and structures that would otherwise be challenging to create using conventional techniques can be completed. In this method, semi-melted plastic wire is the input material. The appropriate shape is created by depositing the material layer by

* Corresponding author
*E-mail addresses:* aamirsharif120@gmail.com.
DOI: 10.5281/zenodo.8020527
Received: 19 January 2023 / Accepted: 03 April 2023
ISSN: 2822-6054 

layer using a nozzle in the 3D digital mode [2, 3]. FDM technology has been used to create a variety of medical applications, including customized surgical guides [4], tissue engineering scaffolds [5], customized implants [6], etc. ABS and PLA are the most widely utilized materials for AM [7, 8]. Amorphous semi-crystalline polymer PLA has a high glass transition temperature (55–60 Co), is highly stable, environmentally friendly, recyclable, and odorless, making it the perfect material for the production of disposable components that are free of contaminants for a variety of applications and industries [9, 10].

Numerous studies focused on PLA material qualities and determined the various properties of the materials through FDM. Chacon et al. [11] studied different manufacturing factors on the mechanical characteristics of PLA samples. Tymark et al. [12] Identify several geometrical factors, such as the raster angle and the distance between extruded filaments that influence the PLA material properties. Levenhagen et al. [13] significantly improved layer adhesion and produced a more isotropic component using bimodal blends with various molecular weights. Ravi et al. [14] studied pre-deposition that causes the temperature at the inter-layer interface to rise, enhancing interpenetrating diffusion and bond strength. Gkartzou et al. [15] demonstrated the usage of a bio-thermoplastic material created with PLA, evaluated various lignin concentrations, and concluded that 5 % weight content was ideal.

In previous studies, limited studies were performed on the inclusion of PLA; therefore, in the current work, different parametric parameters were added to the PLA matrix. The novelty of the current study is to optimize and investigate the influence of the parametric levels used in the current work. This work deals with the process parameter optimization and the effect of each parameter on the impact strength of the PLA material using the FDM technique. An L9 orthogonal array and the Taguchi optimization method were used to optimize the process parameters. The percentage contribution of each process parameter on response was examined using Analysis of variance. The current study aims to optimize the process parameters, investigate the percentage contribution of each input parameter, and evaluate the mechanical properties of PLA.

## 2. Material and Method

### *2.1 Material and equipment*

PLA is the most widely used material in 3D printing technologies and is examined in the current study to see how well the components' mechanical performance performed. A polymer made from lactic acid called PLA is biodegradable. This material's primary benefits are its simplicity and high-quality output for 3D printing. It also does not suffer from significant printing distortions. While printing, it does not emit any unpleasant odors or dangerous fumes. Because PLA tends to distort at temperatures over 60 $C^{o}$, it must not be utilized for components that must tolerate high temperatures. The mechanical properties of PLA filament are shown in Table 1.

**Table 1.** Mechanical properties of PLA filament

| Properties | | Values |
|---|---|---|
| Density | $g/cm^3$ | 1.25 |
| Modulus of Elasticity | Gpa | 3.5 |
| Tensile strength | Mpa | 51 |
| Nominal strain at break | % | 6 |

The MakerBot Marriala 3D printer, which uses FDM technology, will be used for additive manufacturing, as shown in Figure 1. The samples are imported to G-code using the Makerbot printer software. Table 2 lists the MakerBot Marriala 3D printer's primary technical specifications.

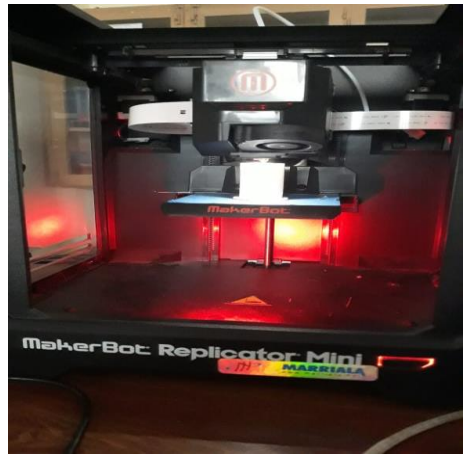


**Fig 1.** Fused deposition modeling process

**Table 2.** Characteristics of the FDM

| Characteristics | | Values |
|---|---|---|
| Resolution | g/cm$^3$ | 0.1 |
| Nozzle diameter | mm | 1.75 |
| Firmware | - | Marlin |
| Maximum printing volume | mm$^3$ | 110 (X) x 100 (Y) x 90 (Z) |
| Maximum printing speed | mm/s | 200 |

*2.2 Impact strength*

The Charpy hammer (Web Werkstoffprüfmaschinen, Leipzig, Germany) was used to assess the impact on the specimens, as shown in Figure 2. The beginning information was as follows: the hammer weight was 6.8 kg, the pendulum's length was 380 mm, and the initial potential energy was 49 J. The following relation was used to calculate the Charpy impact strength (kJ/m²) for samples from the wing leading edges [16].

$$a_{CU} = \frac{E_c}{d.b}.10^3 \qquad (1)$$

Where d is the specimen's thickness (50 mm), b is its width (45.7 mm), and $E_c$ is the energy (J) absorbed by breaking leading edges of the specimens.


**Fig 2.** Experimental set up (Impact Testing)

*2.3 Design of experiments and analysis of variance*

The experiment design examines the behavior of two or more components and affects the most critical levels [17-19]. This study's factor includes layer thickness, infill density, and printing speed, as shown in Table 3. As needed for this study, three levels were considered for each element, as shown in Table 3. In order to determine how much each input parameter affects the response, ANOVA was utilized. ANOVA is a tool for making decisions that help determine the importance of process parameters and how they interact with the response [20-23]. An ANOVA was conducted using a 95% confidence interval [24-26]. P values validate the impact of process factors on responses [27, 28] . Additionally, percentage contribution provided information on how each process parameter affected the responses [29] .

**Table 3** Factor and level for the current study

| **Factors** | | **Levels** | | |
|---|---|---|---|---|
| Layer thickness | (mm) | 0.1 | 0.3 | 0.5 |
| Printing speed | (mm/s) | 60 | 100 | 140 |
| Infill density | (%) | 40 | 60 | 80 |

## 3. Results and Discussion

*3.1 Effect of infill density, layer thickness and printing speed on impact strength*

The impact tests of 27 specimens were determined using equation 1. Figure 3 describes the effect of infill density ($\boldsymbol{d_i}$) and printing speed ($\boldsymbol{s_p}$) on impact strength ($\boldsymbol{s_i}$) of the desired specimens, which were between 12.45 kj/m$^2$ to 22.56 kj/m$^2$. The impact tested samples revealed a total failure. Increasing $\boldsymbol{d_i}$ from 40 % to 80 % increases the strength of the specimens. However, it can be seen from Fig 3 that the ($\boldsymbol{s_i}$) value of the specimens decreases as the $\boldsymbol{s_p}$ rises from 60 mm/s to 140 mm/s. The increase in strength of the specimens by increasing $\boldsymbol{d_i}$ is due to the following reason. When the $\boldsymbol{d_i}$ reached 80 %, there was no space between the printed layer, and each layer began to connect with one above it. The ability of printed layers to bend and absorb stress before breaking in the bond between various layers increased, which also increased the samples $\boldsymbol{s_i}$. A greater $\boldsymbol{s_p}$ would result in a smaller extrusion volume of melting materials and less printing stability, which would result in a decrease in sample strength. The $\boldsymbol{s_p}$ of 100 mm/s allows the melting

material extruded from the nozzle to have efficient time to fuse with the surrounding printed samples, enhancing the improvement of the manufacturing parts [30].

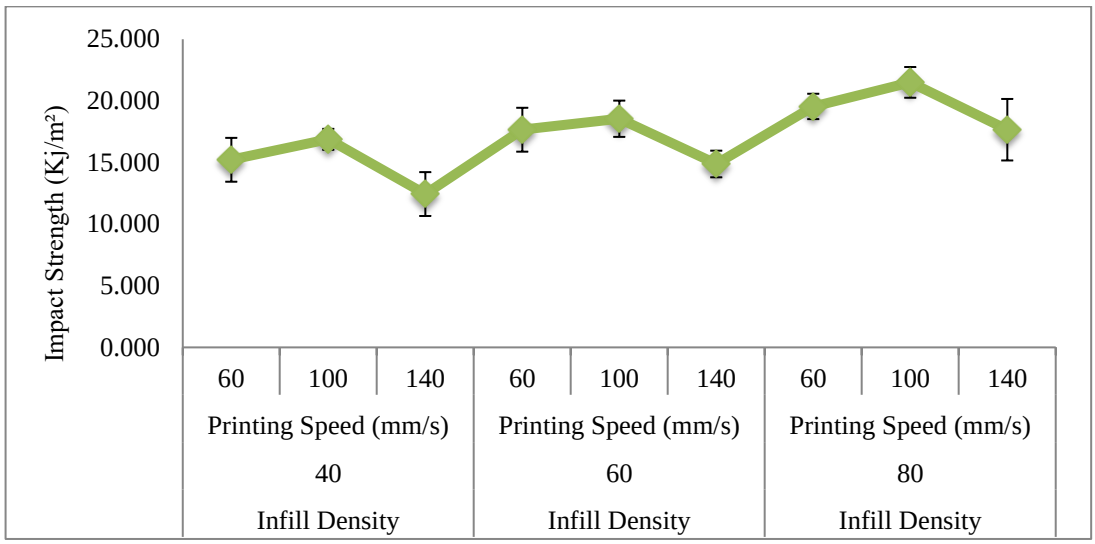


**Fig 3.** Effect of Infill density and Printing speed on Impact strength

The $s_i$ of printed specimens using all levels of $l_t$ varies from 0.1 mm to 0.5 mm are shown in Figure 4. The $s_i$ decrease within the increase in $l_t$. The specimen having $d_i$ of 80 % and $l_t$ of 0.1 have maximum $s_i$ of 22.12 Kj/m$^2$.The nozzle squeezes the deposited filaments to firmly combine the interlamination at 0.1 mm $l_t$, producing a high strength bond. Increasing thickness of the layer has an adverse impact on the mechanical properties of the sample and the strength of the sample reduced by 19 % as the $l_t$ increase from 0.1 mm to 0.5 mm. However, a further increase in $l_t$ after 0.5 mm while utilizing a nozzle with a diameter of 0.6 mm would result in simpler stratification between layers due to a lower squeezing effect induced by the nozzle. Several pores and clear layer boundary absorb on the cross section of the sample with a $l_t$ of 0.5 mm [30].

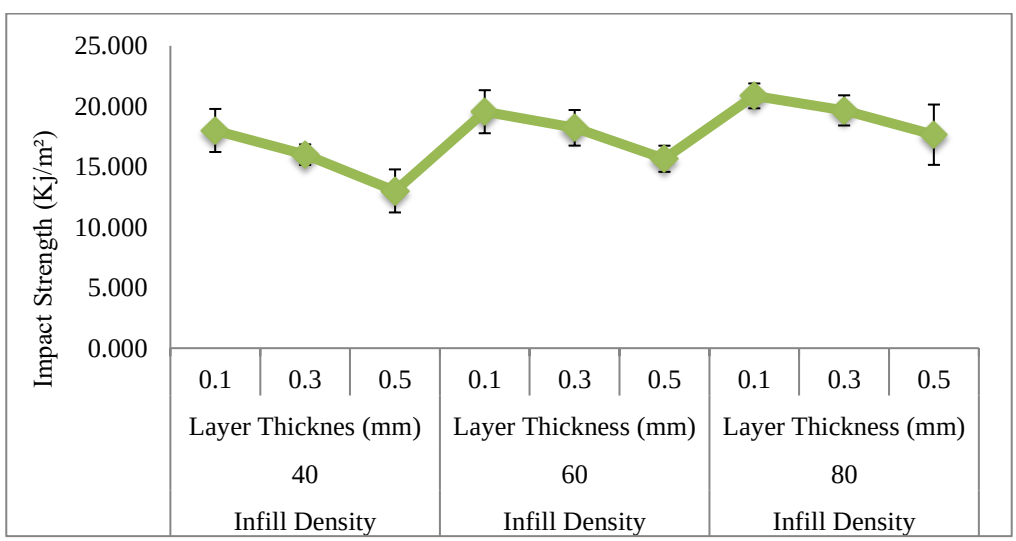


**Fig 4.** Effect of Infill density and Layer thickness on Impact strength

Figure 5 shows the effect of $l_t$ and $s_p$ on $s_i$ of the specimen. The $s_i$ of the specimen decreases with increasing both $l_t$ and $s_p$. Increasing $l_t$ from 0.1 mm to 0.5 mm, the $s_i$ of a sample decreases by 19 %. The decrease in $s_i$ of PLA sample is due to the thicker extrusion of layers that adversely affect the strength of a PLA sample. Additionally, increasing $s_i$ from 60 mm/s to 140 mm/s also decreases the $s_i$ of a PLA sample. The decrease in $s_i$ of PLA samples is due to the gradually expanding of 3D printers that result in low quality fabricated parts. Moreover, higher $s_p$ decreases the mass of the sample as well as decreases the hardness of the top surface of the PLA sample.

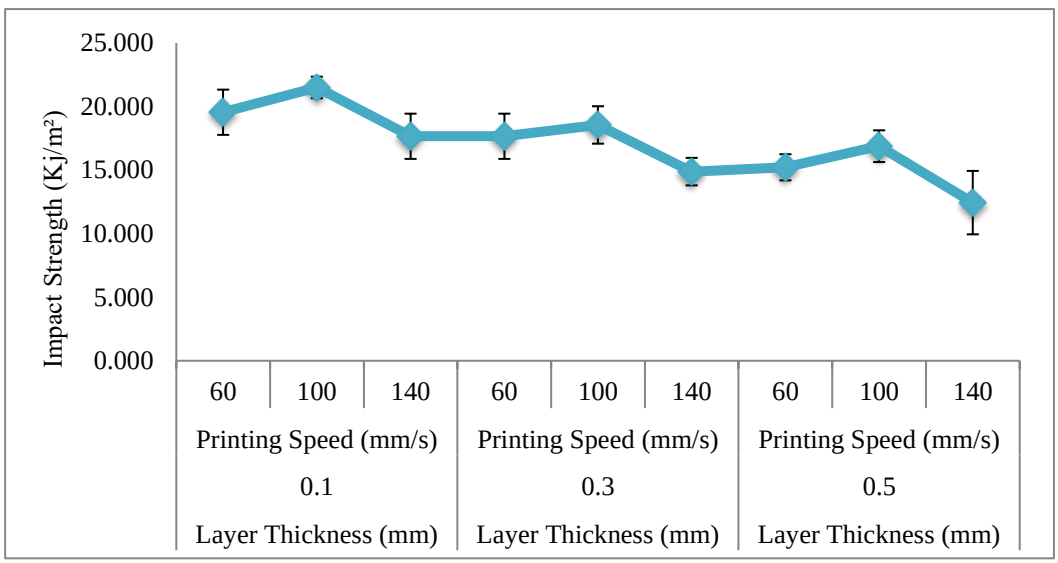


**Fig 5.** Effect of Layer thickness and Printing speed on Impact strength

ANOVA investigated the most affecting parameter and the contribution of each printing parameter. In this instance, the fabricated PLA sample's impact strength is taken into consideration as an output response. ANOVA shows in table 4 that the percentage contribution of $d_i$ is 47.09 % greater than the percentage contribution of $l_t$ and $s_p$ having percentage contribution of 40.14 % and 10.29 %, respectively. Moreover, P-values in Table 3 show that $d_i$ is most significant parameters in selecting parameter in FDM. Moreover, $l_t$ also shows significance while the effect of $s_p$ is less significant.

**Table 4.** Analysis of Variance

| Source | DF | Seq SS | Contribution | Adj SS | Adj MS | F-Value | P-Values |
|---|---|---|---|---|---|---|---|
| Infill density | 2 | 67.169 | 47.09 % | 67.169 | 33.584 | 17.81 | 0.023 |
| Layer thickness | 2 | 65.723 | 40.14 % | 65.723 | 32.861 | 17.42 | 0.034 |
| Printing speed | 2 | 15.671 | 10.29 % | 15.671 | 7.836 | 4.15 | 0.056 |
| Error | 2 | 3.772 | 2.48 % | 3.772 | 1.886 | - | |
| Total | 8 | 152.334 | 100 % | - | - | - | |

### *3.2 Optimization of parametric parameters using Taguchi techniques*

Taguchi analysis has been widely used in engineering and design [31]. The current study used Taguchi analysis to optimize parametric parameters to achieve better quality. The experimental results are converted into an S/N ratio, and the smaller, better model given in Equation (1) is used to evaluate and determine the optimal values for the performance characteristics, such as impact strength. Table 4 shows the average response value and Single to Noise ratio response values. Figure 6 shows the Mean of Means for impact strength of the PLA samples by varying the process parameters such as $d_i$, $l_t$, and $s_p$.

Table 5 displays the $s_i$ response factor for $d_i$, at different values, including 40%, 60%, and 80%. The $d_i$ of 80% resulted in the maximum signal-to-noise ratio value of 26.9 Kj/m$^2$. In this instance, the maximum $s_i$ was found on the highest $d_i$ without considering the printed sample's density into account. There is no space between each layer due to higher $d_i$, and the bonding between layers was strong. As a result, a continuous layer of resin is created that is stronger and can sustain more significant stress before breaking under higher load than under condition with lower $d_i$. The S/N ratio was lower for the 40 % $d_i$ when the density of the printed component was taken into account. This is because the material which can sustain a particular equivalent load value for the 80% $d_i$ samples loses density at lower $d_i$ conditions. This demonstrates clearly that considering components density, the $d_i$ significantly affects the output response of polymer samples. Similar findings have been made by Aw et al. [32] who found that the $d_i$ had a significant impact on the ABS/Zno composite strength.

In addition, Table 5 displays the factor of $l_t$, for the $s_i$ response under various processing settings, includin g 0.1 mm, 0.3 mm, and 0.5 mm. At a $l_t$ of 0.1 mm, the maximum signal-to noise ratio value for the $s_i$ of PLA polymer is 24.89 Kj/m$^2$. As the $l_t$ decrease, there is a possibility of a significant interface gap forming between each layer, which makes it easier for material to readily slide from one layer to another layer that, lowers the $s_i$. Similarly, as $l_t$ increases, the number of layers decreases, making it difficult to effectively transfer loads from one layer to the next layer. The 0.5 mm layer has weaker impact strength than 0.3 mm layer. The impact of different process conditions on optimizing fused deposition modeling techniques was examined by Sood et al.[33]. The results are consistent with the $l_t$ of the experimental results.

Moreover, table 5 also illustrates the influence of the $s_p$ on the $s_i$ at various printing speeds of 60 mm/s, 100 mm/s, and 140 mm/s. The finding indicates that 23.89 Kj/m$^2$ is the maximum value for the signal-to-noise ratio for the $s_p$ pertaining to the PLA polymer. PLA polymer samples have greater responsiveness to $s_i$ as $s_p$ increases. As the $s_p$ increase up to 100 mm/s, the fusion of each layer is high up to a certain limit that accounts for the improvement in the $s_i$ response. However, as $s_p$ was increased to 140 mm/s, $s_i$ response of the PLA samples decreased. The $s_p$ has less effect than the other two printing parameters. According to the overall experimental findings, $d_i$of 80 %, a minimum $l_t$ of 0.1 mm and $s_p$ of 100 mm/s are the ideal conditions for producing PLA material samples with higher $s_i$.

**Table 5.** Taguchi Analysis

| Average Response Values | | | | S/N Ratio Response Values | | | |
|---|---|---|---|---|---|---|---|
| Impact Strength | | | | | | | |
| Level | Density (%) | Layer Height (mm) | Travel Speed (mm/s) | Level | Density (%) | Layer Height (mm) | Travel Speed (mm/s) |
| 1 | 16.66 | 21.07* | 18.66 | 1 | 22.66 | 24.89* | 22.56 |
| 2 | 18.22 | 20.00 | 21.22* | 2 | 24.22 | 23.66 | 23.89* |
| 3 | 22.18* | 16.00 | 17.18 | 3 | 26.99 | 20.22 | 21.66 |
| Delta | 5.52 | 5.07 | 4.03 | Delta | 1.96 | 1.22 | 0.62 |
| Rank | 1 | 2 | 3 | Rank | 1 | 2 | 3 |

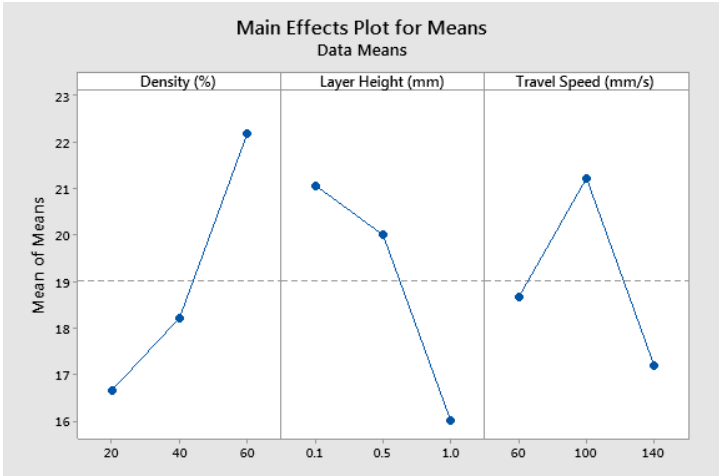


**Fig 6.** Mean of Means of parametric parameters

## 4. Conclusion

Various experimental techniques were employed to investigate the impacts of input parameters to enhance the mechanical properties of PLA generated by FDM based additive manufacturing. Increasing infill density from 40 % to 80 % increases the impact strength of PLA samples. However, increasing layer thickness from 0.1 mm to 0.5 mm decrease the impact strength. Furthermore, the impact strength of PLA samples decreases with increasing printing speed from 60 mm/s to 140 mm/s. From the Taguchi table, the optimal condition for obtaining higher the impact strength will be 80% infill density, 0.1 mm layer thickness, and 100 printing speed. The ANOVA analysis results show that the effect of infill density on impact strength of the specimens is more than layer thickness and printing speed. The percentage contribution of infill density, layer thickness, and printing speed is 47.09 %, 40.14 %, and 10.29 %, respectively. Infill density and layer thickness significantly contribute to obtaining a higher impact strength. However, printing speed follows the minor contribution on sample tests. The crack was absorbed the wall of samples during lower infill density and higher printing speed. Moreover, complete fracture propagation occurred in the vertical direction in case of higher layer thickness.

## Author Contribution Statement

Conceptualization A.S, H.K; methodology, A.S, H.K; investigation, A.S, N.B, W.A; resources, H.K, N.B.; writing—A.S. N.B, writing—review and editing, A.S.; W. A

## Acknowledgements

Manufacturing lab at CECOS University, Pakistan has been a great help and source of assistance for the authors, and they appreciate it very much.

**Conflicts of Interest:** The authors declare no conflict of interest

## References


[1] Brancewicz-Steinmetz, E., Sawicki, J., & Byczkowska, P. (2021). The influence of 3D printing parameters on adhesion between polylactic acid (PLA) and thermoplastic polyurethane (TPU). Materials, 14(21), 6464.

[2] Özen, A., Auhl, D., Völlmecke, C., Kiendl, J., & Abali, B. E. (2021). Optimization of manufacturing parameters and tensile specimen geometry for fused deposition modeling (FDM) 3D-printed PETG. Materials, 14(10), 2556.

[3] Verdejo de Toro, E., Coello Sobrino, J., Martínez Martínez, A., Miguel Eguía, V., & Ayllón Pérez, J. (2020). Investigation of a short carbon fibre-reinforced polyamide and comparison of two manufacturing processes: Fused Deposition Modelling (FDM) and polymer injection moulding (PIM). Materials, 13(3), 672.

[4] Popescu, D., Laptoiu, D., Marinescu, R., & Botezatu, I. (2018). Design and 3D printing customized guides for orthopaedic surgery–lessons learned. Rapid Prototyping Journal, 24(5), 901-913.

[5] Shuai, C., Shuai, C., Wu, P., Yuan, F., Feng, P., Yang, Y., ... & Gao, C. (2016). Characterization and bioactivity evaluation of (polyetheretherketone/polyglycolicacid)-hydroyapatite scaffolds for tissue regeneration. Materials, 9(11), 934.

[6] Fukuda, H. (2015). Additive manufacturing technology for orthopedic implants. Advances in Metallic Biomaterials: Processing and Applications, 3-26.

[7] Van den Eynde, M., & Van Puyvelde, P. (2018). 3D Printing of Poly (lactic acid). Industrial Applications of Poly (lactic acid), 139-158.

[8] Ahmed, M., Islam, M., Vanhoose, J., & Rahman, M. (2017). Comparisons of elasticity moduli of different specimens made through three dimensional printing. 3D Printing and additive manufacturing, 4(2), 105-109.

[9] García Plaza, E., López, P. J. N., Torija, M. Á. C., & Muñoz, J. M. C. (2019). Analysis of PLA geometric properties processed by FFF additive manufacturing: Effects of process parameters and plate-extruder precision motion. Polymers, 11(10), 1581.

[10] Rodríguez-Panes, A., Claver, J., & Camacho, A. M. (2018). The influence of manufacturing parameters on the mechanical behaviour of PLA and ABS pieces manufactured by FDM: A comparative analysis. Materials, 11(8), 1333.

[11] Chacón, J. M., Caminero, M. A., García-Plaza, E., & Núnez, P. J. (2017). Additive manufacturing of PLA structures using fused deposition modelling: Effect of process parameters on mechanical properties and their optimal selection. Materials & Design, 124, 143-157.

[12] Tymrak, B. M., Kreiger, M., & Pearce, J. M. (2014). Mechanical properties of components fabricated with open-source 3-D printers under realistic environmental conditions. Materials & Design, 58, 242-246.

[13] Levenhagen, N. P., & Dadmun, M. D. (2018). Interlayer diffusion of surface segregating additives to improve the isotropy of fused deposition modeling products. Polymer, 152, 35-41.

[14] Ravi, A. K., Deshpande, A., & Hsu, K. H. (2016). An in-process laser localized pre-deposition heating approach to inter-layer bond strengthening in extrusion based polymer additive manufacturing. Journal of Manufacturing Processes, 24, 179-185.

[15] Gkartzou, E., Koumoulos, E. P., & Charitidis, C. A. (2017). Production and 3D printing processing of bio-based thermoplastic filament. Manufacturing Review, 4, 1.

[16] ISO, I., (2010), Plastics—Determination of Charpy Impact Properties, Part 1: Non-Instrumented Impact Test. International Organization for Standardization: Geneva, Switzerland.

[17] Habib, N., Sharif, A., Hussain, A., Aamir, M., Giasin, K., Pimenov, D. Y., & Ali, U. (2021). Analysis of hole quality and chips formation in the dry drilling process of Al7075-T6. Metals, 11(6), 891.

[18] Sharif, A., Siddiqi, M. U. R., Tahir, M., Ullah, U., Noon, A. A., Muhammad, R., ... & Sheikh, N. A. (2021). Investigating the Effect of Inlet Head and Water Pressure on the Performance of Single Stage Gravitational Water Vortex Turbine. Journal of Mechanical Engineering Research and developments, 44(11), 156-168.

[19] Tipu, A. K., Arif, M., Sharif, A., & Siddiqi, M. U. R. (2021). Implementing Truss Elements for Ensuring Structural Integrity on the Blade of Up-scaled Gravitational Water Vortex Turbine. J. Mechan. Engin. Res. Develop, 44, 115-122.

[20] Kowalczyk, M. (2014). Application of Taguchi and Anova methods in selection of process parameters for surface roughness in precision turning of titanium. Advances in Manufacturing Science and Technology, (2).

[21] Habib, N., Sharif, A., Hussain, A., Aamir, M., Giasin, K., & Pimenov, D. Y. (2022). Assessment of hole quality, thermal analysis, and chip formation during dry drilling process of gray cast iron ASTM A48. Eng, 3(3), 301-310.

[22] Hussain, A., Sharif, A., Habib, N., Ali, S., Akhtar, K., Ahmad, F., ... & Ishaq, M. (2021). Effect of Drilling Process Parameters on Brass Alloy 272 Through Experimental Techniques. Journal of Mechanical Engineering Research and Developments, 44(11), 222-234.

[23] Shoukat, A. A., Noon, A. A., Anwar, M., Ahmed, H. W., Khan, T. I., Koten, H., ... & Sharif, A. (2021). Blades Optimization for Maximum Power Output of Vertical Axis Wind Turbine. International Journal of Renewable Energy Development, 10(3).

[24] Neseli, S. (2014). Optimization of process parameters with minimum thrust force and torque in drilling operation using Taguchi method. Advances in Mechanical Engineering, 6, 925382.

[25] Sharif, A. (2022). Study on burr formation, tool wear and surface quality in machining Al6063. Journal of Materials and Manufacturing, 1(2), 1-9.

[26] Sharif, A., Siddiqi, M., & Muhammad, R. (2020). Novel runner configuration of a gravitational water vortex power plant for micro hydropower generation. Journal of Engineering and Applied Sciences, 39(1), 87-93.

[27] Ullah, I., & Sharif, A. (2022). Novel Blade Design and Performance Evaluation of a Single-Stage Savanious Horizontal Water Turbine. Journal of Technology Innovations and Energy, 1(4), 42-50.

[28] Sharif, A., Tipu, J. A. K., Arif, M., Abbasi, M. S., Jabbar, A. U., Noon, A. A., & Siddiqi, M. U. R. (2022). Performance Evaluation of a Multi-Stage Gravitational Water Vortex Turbine with optimum number of Blades. J. Mechan. Engin. Res. Develop, 45, 35-43.

[29] Ullah, I., Siddiqi, M. U. R., Tahir, M., Sharif, A., Noon, A. A., Tipu, J. A. K., ... & Habib, T. (2022). Performance Investigation of a Single-Stage Savanious Horizontal Water Turbine with Optimum Number of Blades. Journal of Mechanical Engineering Research and Developments, 45(2), 29-42.

[30] Peng, W. A. N. G., Bin, Z. O. U., Shouling, D. I. N. G., Lei, L. I., & Huang, C. (2021). Effects of FDM-3D printing parameters on mechanical properties and microstructure of CF/PEEK and GF/PEEK. Chinese Journal of Aeronautics, 34(9), 236-246.

[31] Taguchi, G. (1990). Introduction to quality engineering, Tokyo. Asian Productivity Organization, 4(2), 10-15.

[32] Aw, Y. Y., Yeoh, C. K., Idris, M. A., Teh, P. L., Hamzah, K. A., & Sazali, S. A. (2018). Effect of printing parameters on tensile, dynamic mechanical, and thermoelectric properties of FDM 3D printed CABS/ZnO composites. Materials, 11(4), 466.

[33] Sood, A. K., Ohdar, R. K., & Mahapatra, S. S. (2012). Experimental investigation and empirical modelling of FDM process for compressive strength improvement. Journal of Advanced Research, 3(1), 81-90.